Journal of Quantitative Spectroscopy & Radiative Transfer 218 (2018) 178–186

Contents lists available at ScienceDirect

Journal of Quantitative Spectroscopy & Radiative Transfer

journal homepage: www.elsevier.com/locate/jqsrt

# MARVEL analysis of the measured high-resolution rovibrational spectra of $H_2{}^{32}S$

Katy L. Chubb[a,*], Olga Naumenko[b], Stefan Keely[c], Sebestiano Bartolotto[c], Skye Macdonald[c], Mahmoud Mukhtar[c], Andrey Grachov[c], Joe White[c], Eden Coleman[c], Anwen Liu[d], Alexander Z. Fazliev[b], Elena R. Polovtseva[b], Veli-Matti Horneman[e], Alain Campargue[f], Tibor Furtenbacher[g], Attila G. Császár[g], Sergei N. Yurchenko[a], Jonathan Tennyson[a]

[a] Department of Physics and Astronomy, University College London, London WC1E 6BT, UK
[b] V. E. Zuev Institute of Atmospheric Optics, Siberian Branch Russian Academy of Sciences, Tomsk, Russia
[c] Highams Park School, Handsworth Avenue, Highams Park, London E4 9PJ, UK
[d] Hefei National Laboratory for Physical Sciences at Microscale, University of Science and Technology of China, Hefei 230026, China
[e] Department of Physics, University of Oulu, P.O. Box 3000, FIN-90014, Finland
[f] Université Grenoble Alpes, CNRS, LIPhy, Grenoble F-38000, France
[g] Institute of Chemistry, Eötvös Loránd University and MTA-ELTE Complex Chemical Systems Research Group, H-1518 Budapest 112, P.O. Box 32, Hungary

ARTICLE INFO

*Article history:*
Received 15 April 2018
Revised 3 July 2018
Accepted 16 July 2018
Available online 19 July 2018

*Keywords:*
Spectroscopy
Energy levels
Hydrogen sulfide

ABSTRACT

44 325 measured and assigned transitions of $H_2{}^{32}S$, the parent isotopologue of the hydrogen sulfide molecule, are collated from 33 publications into a single database and reviewed critically. Based on this information, rotation-vibration energy levels are determined for the ground electronic state using the Measured Active Rotational-Vibrational Energy Levels (MARVEL) technique. The *ortho* and *para* principal components of the measured spectroscopic network of $H_2{}^{32}S$ are considered separately. The verified set of 25 293 *ortho*- and 18 778 *para*- $H_2{}^{32}S$ transitions determine 3969 *ortho* and 3467 *para* energy levels. The MARVEL results are compared with alternative data compilations, including a theoretical variational linelist.



## 1. Introduction

Hydrogen sulfide, $H_2S$, is a volcanic gas present on earth and other geologically active planets and moons, such as Io [1], Venus [2], and, theoretically, hot super-earth "lava" exoplanets [3]. It has recently been detected above the clouds in the atmosphere of Uranus [4]. On earth, microbial respiration of seawater sulfate creates a hydrogen sulfide-rich ecosystem [5], suggesting that $H_2S$ is a component for a potential microbial life sustaining atmosphere on Venus [2], and a potential biomarker for life on exoplanets [6]. $H_2S$ influences many physiological processes [7], it is of importance in the treatment of respiratory diseases [8], and it is used as a measure of the quality of air near oil refineries [9]. The parent isotopologue, $H_2^{32}S$, was first detected in interstellar space in 1972 [10]. Many of the scientific and engineering applications mentioned require the detailed knowledge of the rovibrational energy levels of $H_2{}^{32}S$.

As part of this work, we present the largest compilation of published experimental rovibrational transition data for $H_2^{32}S$. The experimental database of $H_2^{32}S$ transitions has been formatted and analysed using the MARVEL (Measured Active Rotational-Vibrational Energy Levels) spectroscopic network (SN) software [11–13]. This study builds on the data of the 2012W@DIS information system for the hydrogen sulfide molecule [14].

As to the structure of this paper, the next section provides the theory underlying the present study. Section 3 presents and discusses the experimental sources used, with results given in Section 4. Section 5 discusses these results and compares the empirical rovibrational energies presented in this work with corresponding levels previously determined both by experiment and theory. Finally, Section 6 provides our conclusions. All transition data and energy levels resulting from this work are included as supplementary data files.

* Corresponding author.
*E-mail addresses:* katy.chubb.14@ucl.ac.uk (K.L. Chubb), j.tennyson@ucl.ac.uk (J. Tennyson).

https://doi.org/10.1016/j.jqsrt.2018.07.012

## 2. Theory

### 2.1. MARVEL

The MARVEL procedure [11–13] is based on the theory of spectroscopic networks [15,16], with the energy levels represented as nodes and the transitions between them as edges. The related MARVEL code can be used to critically evaluate and validate experimentally-determined transition wavenumbers and uncertainties collected from the literature, inverting the wavenumber information to obtain accurate empirical energy levels with an associated uncertainty. MARVEL has been successfully used to evaluate the energy levels for molecules such as $^{12}C_2$ [17], $^{48}Ti^{16}O$ [18], water vapour [19–23], $H_3^+$ [24], $H_2D^+$ and $D_2H^+$ [25], $^{12}C_2H_2$ [26], $^{14}NH_3$ [27,28], and $^{12}C_2H_2^{16}O$ [29]. MARVEL requires each measured transition to have an associated uncertainty and for each energy level considered to possess a unique set of quantum numbers.

### 2.2. Quantum number labelling

The seven quantum numbers that were used for labelling the upper and lower rovibrational states of $H_2^{32}S$ are the same as those used in a previous MARVEL investigation to classify water [19]. These quantum numbers are summarised in Table 1. Normal-mode labelling is used for the vibrations, where $\nu_1$, $\nu_2$ and $\nu_3$ stand for the symmetric stretch, bend, and antisymmetric stretch vibrations, respectively. Standard asymmetric-top quantum numbers are used for the rotations, where $J$, $K_a$, and $K_c$ are the three quantum numbers associated with rotational angular momentum, **J**, and the two projections along the $A$ and $C$ axes. We also provide, as part of the label, the nuclear spin state (*ortho* or *para*), which is deduced by whether $(\nu_3 + K_a + K_c)$ is odd (*ortho*) or even (*para*) [26,30]. Hyperfine coupling associated with nuclear spins has been neglected.

When local-mode notation was used by an experimental source considered in this work, the quantum numbers were transformed to the normal-mode notation $(\nu_1\nu_2\nu_3)$ to describe a vibrational state. Note that some of the data sources considered in this study use $J$ and $\tau = K_a - K_c$ instead of $J$, $K_a$, and $K_c$ [31], where $\tau$ runs from $-J, -J+1, \ldots, J-1, +J$, with energy increasing from $\tau = -J$. The $+/-$ parity of an asymmetric top molecule such as $H_2^{32}S$ is defined by $(-1)^{K_c}$ [19]. $H_2^{32}S$ belongs to the $C_{2v}$(M) molecular symmetry (MS) group [32], which contains irreducible representations $A_1$, $A_2$, $B_1$, and $B_2$, as given in Table 2.

### 2.3. Selection rules

The rigorous selection rules governing rotation-vibration transitions for a molecule of the $C_{2v}$(M) MS group are given by:

$$\Delta J = 0, \pm 1, \tag{1}$$

$$J' + J'' \neq 0, \tag{2}$$

$$- \leftrightarrow + \tag{3}$$

**Table 1**
Quantum numbers used to label the upper and lower energy states of $H_2^{32}S$.

| Label | Description |
|---|---|
| $v_1$ | S-H symmetric stretch ($\sim$2614.4 cm$^{-1}$) |
| $v_2$ | Symmetric bending mode ($\sim$1182.6 cm$^{-1}$) |
| $v_3$ | S-H antisymmetric stretch ($\sim$2628.5 cm$^{-1}$) |
| $J$ | Rotational angular momentum |
| $K_a$, $K_c$ | Projections of rotational angular momentum |
| *ortho*/*para* | Nuclear spin state (see text) |

**Table 2**
Symmetry of the rovibrational states of $H_2^{32}S$.

| Symmetry | $A_1$ | $A_2$ | $B_1$ | $B_2$ |
|---|---|---|---|---|
| Parity | + | - | - | + |
| Nuclear spin state | *para* | *para* | *ortho* | *ortho* |

The *ortho* states of $H_2^{32}S$ have the nuclear spin statistical weight $g_{ns} = 3$, while for the *para* states $g_{ns} = 1$, thus, *ortho* transitions have three times the intensity of *para* transitions. This is sometimes referred to as intensity alternation. It is assumed that *ortho* and *para* states do not interconvert. Such transitions are very weakly allowed [33] but have yet to be observed for $H_2^{32}S$.

## 3. Experimental sources

A large number of experimentally determined transition wavenumbers can be found in the literature for the main isotopologue of hydrogen sulfide, $H_2^{32}S$. We have attempted to conduct a rigorous and comprehensive search for all useable spectroscopic data. Fortunately, much of the data up to 2012 was previously collated as part of the 2012 W@DIS information system for hydrogen sulfide [14], in which some of the authors of this paper were involved. These data were converted to MARVEL format for this work and analysed alongside data from newly collected sources. This requires the transition wavenumber (in cm$^{-1}$) and the associated uncertainty, along with quantum number assignments for both the upper and lower energy states, and a unique reference label for each transition. This reference indicates the data source the transition originates from. The data source tag is based on the notation employed by an IUPAC Task Group on water spectroscopy [19]. An extract of the input file in the required format is given in Table 3; the full file can be found in the supplementary data for this publication.

33 sources of experimental data were used in the final data set. The data from more recent papers are generally provided in digital format, but some of the older papers had to be processed through digitalisation software, or even manually entered in the worst cases. After digitalisation the data were converted to MARVEL format, as described above.

Table 4 gives a summary of all the data sources used in this work, along with the energy range, number of transitions (as-

**Table 3**
Extract from the MARVEL input file for the *ortho* transitions for $H_2^{32}S$. The full file is supplied as part of the supplementary information to this paper. All energy term values and uncertainties are in units of cm$^{-1}$. The meaning of the upper and lower state assignments can be found in Table 1.

| Transition | Uncertainty | Upper state assignment | Lower state assignment | Reference |
|---|---|---|---|---|
| 33.12631 | 0.00015 | 0 0 0 5 2 3 ortho | 0 0 0 5 1 4 ortho | 94YaKl_1 |
| 33.12631 | 0.00018 | 0 0 0 3 0 3 ortho | 0 0 0 2 1 2 ortho | 94YaKl_2 |
| 34.00529 | 0.00010 | 0 0 0 8 7 2 ortho | 0 0 0 8 6 3 ortho | 94YaKl_5 |
| 34.15779 | 0.00010 | 0 0 0 11 9 2 ortho | 0 0 0 11 8 3 ortho | 94YaKl_7 |
| 34.21980 | 0.00010 | 0 0 0 6 4 3 ortho | 0 0 0 6 3 4 ortho | 94YaKl_8 |
| 34.24062 | 0.00012 | 0 0 0 4 2 3 ortho | 0 0 0 4 1 4 ortho | 94YaKl_9 |
| 35.73512 | 0.00010 | 0 0 0 8 6 3 ortho | 0 0 0 8 5 4 ortho | 94YaKl_13 |

**Table 4**
Data sources used in this study with frequency range, numbers of transitions (A/V for assigned/verified), and comments, which are detailed in Section 3.1. As far as we are aware all experiments were conducted at room temperature.

| Tag | Ref. | Range ($cm^{-1}$) | A/V | Comments |
|---|---|---|---|---|
| 72HeCoLu | [34] | 1.17–25.55 | 37/35 | (4a) |
| 95BeYaWiPo | [35] | 4.39–85.41 | 112/84 | (4b) |
| 68CuKeGa | [36] | 5.63–14.15 | 6/6 | |
| 71Huiszoon | [37] | 5.63–7.23 | 2/2 | |
| 14CaPu | [38] | 7.23–53.17 | 70/70 | |
| 85BuFeMeSh | [39] | 10.02–20.9 | 6/6 | |
| 94YaKl | [40] | 33.13–259.76 | 366/366 | |
| 13CaPu | [41] | 33.97–37.45 | 4/4 | |
| 13AzYuTeMa | [42] | 45.25–359.79 | 1158/1139 | (4c) |
| 83FlCaJo | [43] | 50.77–307.51 | 426/387 | (4d) |
| 18UlBeGr | [44] | 729.78–1735.41 | 2267/2267 | |
| 82LaEdGiBo | [45] | 1003.46–1495.28 | 397/396 | (4e) |
| 83Strow | [46] | 1082.03–1257.07 | 123/123 | |
| 96UlMaKoAl | [47] | 1178.05–1359.78 | 41/41 | |
| 98BrCrCrNa | [48] | 2141.30–4249.85 | 7473/7473 | |
| 18Horneman | [49] | 2180.35–4220.46 | 4460/4460 | |
| 84LeFlCaJo | [50] | 2180.36–2945.81 | 2113/2111 | (4f) |
| 81GiEd | [51] | 2192.48–2823.11 | 715/704 | (4g) |
| 96UlOnKoAl | [52] | 3614.70–3887.66 | 106/106 | |
| 05UlLiBeGr | [53] | 4000.59–6653.79 | 2347/2347 | |
| 97BrCrCrNa | [54] | 4500.88–5595.01 | 5221/5219 | (4h) |
| 18Liu | [55] | 4514.79–5555.58 | 3337/3335 | (4i) |
| 04BrNaPoSi_c | [56] | 5688.27–6676.71 | 3178/3178 | |
| 04BrNaPoSi_a | [57] | 7169.19–7898.97 | 2878/2876 | (4j) |
| 04UlLiBeGr_b | [58] | 7226.81–7994.09 | 1855/1855 | |
| 04UlLiBeGr_a | [59] | 8405.91–8905.28 | 589/589 | |
| 04BrNaPoSi_b | [60] | 8412.73–8906.11 | 1179/1175 | (4k) |
| 03DiNaHuZh | [61] | 9541.01–10000.71 | 1736/1728 | (4l) |
| 01NaCa_a | [62] | 10787.33–11297.99 | 1105/1097 | (4m) |
| 94GrRaStDe | [63] | 11948.91–12246.28 | 227/145 | (4n) |
| 97VaBiCaFl | [64] | 12324.55–12670.68 | 399/387 | (4o) |
| 99CaFl | [65] | 13060.51–13357.14 | 219/206 | (4p) |
| 01NaCa_b | [66] | 16186.25–16436.57 | 173/154 | (4q) |
| Total | | 1.17–16436.57 | 44 325/44 071 | |

signed (A) and verified (V)), and comments, which are detailed in Section 3.1. Table 5 lists those data sources which were considered but not used, with comments on the reasons for their exclusion from the analysis. The reference tag given in these tables matches those used in the unique labels in the MARVEL input files, given in the supplementary data and illustrated in Table 3.

As transitions have never been observed between *ortho* and *para* states of $H_2^{32}S$, they form two separate principal components (PCs) of the experimental spectroscopic network. All input and output files supplied in the supplementary data to this work are split into either *ortho* or *para*.

### 3.1. Comments on the experimental sources of Table 4

**(4a)** 72HeCoLu [34] contains 2 lines which have been cited as taken from other experimental sources, for which the original data are already in our dataset. These duplicates were removed.

**(4b)** 95BeYaWiPo [35] contains 28 lines which have been cited as from other experimental sources, for which the original data are already in our dataset. These duplicates were removed.

**(4c)** 13AzYuTeMa [42] gives data for rotational lines recorded at room temperature. The equipment used provides spectra with very high sensitivity and this enabled transitions between highly rotationally excited states to be recorded, even at room temperature. These high rotational excitations may not be so accurately assigned as those of lower energy, as there are no data from other sources in the same region to confirm these measurements. The supplementary data from the original paper does not contain the original experimental transitions; this was provided by the corresponding author. There were 19 lines which could not be validated against other data and so were removed from our dataset (see Section 3.2).

**(4d)** 83FlCaJo [43] contains 39 lines which have been cited as from other sources which are already present in our dataset. The duplicates were removed.

**(4e)** 82LaEdGiBo [45] contains one line which could not be validated and so has been removed from our dataset.

**(4f)** 84LeFlCaJo [50] contains 2 lines which could not be validated against other more recent data and were removed from our dataset. All data from this source were recalibrated; the calibration factor employed was 0.999 999 746 below 2450 $cm^{-1}$ and 1.000 000 0714 above 2450 $cm^{-1}$.

**(4g)** 81GiEd [51] contains 11 lines which could not be validated against more recent data and thus were removed from our dataset.

**(4h)** 97BrCrCrNa [54] contains 2 lines with no corresponding energy in the AYT2 linelist (see Section 5) and so were removed from our dataset.

**(4i)** 18Liu [55] contains 2 lines with no corresponding energy in the AYT2 linelist and so were removed from our dataset.

**(4j)** 04BrNaPoSi_a [57] contains 2 lines with no corresponding energy in the AYT2 linelist and so were removed from our dataset.

**(4k)** 04BrNaPoSi_b [60] contains 4 lines which could not be validated and were removed from our dataset.

**(4l)** 03DiNaHuZh [61] contains one blended line which has been removed from our dataset. A further 7 lines were found to include

**Table 5**
Data sources considered but not used in this work.

| Tag | Ref. | Comments |
|---|---|---|
| 02CoRoTy | [67] | Data taken from other sources |
| 94WaKuSu | [68] | Data taken from other sources |
| 96SuMeKr | [69] | Data taken from other sources |
| 97SuMeKr | [70] | Data taken from other sources |
| 97Sumpf | [71] | Data taken from other sources |
| 98PiPoCoDe | [72] | Data from http://spec.jpl.nasa.gov. Data does not appear to be experimental. |
| 73HeDeKi | [73] | Data taken from other sources, [34,36,37] |
| 02KiSuKrTi | [74] | Data appears to be taken from the 1996 edition of HITRAN [75] |
| 06Polovtseva | N/A | Thesis, no citation. Referenced in [14] |
| 87LeFlCaAr | [76] | Energy levels |
| 13Azzam | [77] | All results are given in 13AzYuTeMa [42] |
| 94KoJe | [78] | Energy levels |
| 95FlGrRa | [79] | Energy levels |
| 85LaEdGiBo | [80] | Calculated values, compared to experimental values from 83FlCaJo [43] |
| 94ByNaSmSi | [81] | Energy Levels |
| 01TyTaSc | [82] | Vibrational energy Levels |
| 69MiLeHa | [83] | Could not be validated with the other sources to a reasonable accuracy (see Section 3.2) |
| 56AlPl | [31] | Could not be validated with the other sources to a reasonable accuracy (see Section 3.2) |
| 69SnEd | [84] | Could not be validated with the other sources to a reasonable accuracy (see Section 3.2) |

a level with no corresponding energy in the AYT2 linelist and so were removed from our dataset.

**(4m)** 01NaCa_a [62] contains 8 transitions which were found to have no corresponding levels in the AYT2 linelist and so were removed from our dataset.

**(4n)** 94GrRaStDe [63] tentatively assigned the vibrational band in their data as $(\nu_1, \nu_2, \nu_3) = (2, 2, 2)$; however, in 95FlGrRaSt [79], a paper published later with the same authors, the revised assignment is $(\nu_1, \nu_2, \nu_3) = (3, 0, 2)$. We adopt the latter vibrational label in our dataset. No other data sources probe this vibrational band. The frequency is only given to 3 decimal places, so the uncertainty was altered to match. The original dataset has 82 transitions either labelled with an asterisk to indicate lines from the $H_2^{34}S$ isotopologue, or labelled with a dagger to indicate lines which have been perturbed due to those from $H_2^{34}S$ [63]. We have commented these out by adding a minus sign to the wavenumber and added the label *_pt* to the end.

**(4o)** 97VaBiCaFl [64] contains 4 lines which could not be validated and so were removed from our dataset. A further 8 lines were found to contain a level with no corresponding energy in the AYT2 linelist and so were removed from our dataset.

**(4p)** The assignment for 99CaFl_185_na_ct from 99CaFl [65] leads to different spin states (*ortho*/*para*) for the upper and lower state, which is forbidden. We have removed this transition from our dataset. 5 other lines could not be validated and so were removed from our dataset. 7 lines were found to have no variational counterparts in the AYT2 linelist and so were removed.

**(4q)** 01NaCa_b [66] contains one line which could not be validated and so was removed from our dataset. A further 18 lines were found to contain levels with no corresponding energies in the AYT2 linelist and so were removed from our dataset.

### 3.2. General comments

All transitions which were considered but not processed in the final dataset have a minus sign in front of the transition wavenumber (indicating that Marvel will ignore them) in the input files provided as supplementary material and are labelled with a comment at the end of the reference (see the comments of Section 3.1). We used a cut-off of 0.035 $cm^{-1}$ as the largest acceptable uncertainty and removed any transitions with an uncertainty greater than this, with a note in Section 3.1 to indicate how many transitions from a particular data source could not be validated to within this accuracy.

The publications 97BrCrCrNa [54], 04BrNaPoSi_c [56], 04BrNaPoSi_a [57], and 04BrNaPoSi_b [60] include just a short description of the assignment and modelling of the Fourier Transform (FT) spectra between 4500 and 8900 $cm^{-1}$. Detailed information on the theoretical treatment of these spectra will be published separately in due course. Some of these transitions, between 4400–8000 $cm^{-1}$, were previously reported in the HITRAN-2012 [85] and HITRAN-2016 [86] databases, while the second decade region, 8400–8900 $cm^{-1}$, is presented for the first time. It is also worth mentioning that the Marvel dataset includes a considerable number of transitions which include new, unpublished energy levels. As only the upper energy levels of the transitions were reported in 05UlLiBeGr [53], 04UlLiBeGr_b [58], and 04UlLiBeGr_a [59], the corresponding transition wavenumbers were recovered from Liu (18Liu [55]) using the energy levels obtained from 97BrCrCrNa [54], 04BrNaPoSi_c [56], 04BrNaPoSi_a [57], and 04BrNaPoSi_b [60]. For this reason, the transitions in the Marvel dataset which are referred to as from 05UlLiBeGr [53], 04UlLiBeGr_b [58], and 04UlLiBeGr_a [59] contain a larger number of assignments than reported in the original publications. The data of the first hexad region between 4500–5600 $cm^{-1}$ were totally assigned based on the energy levels reported in 97BrCrCrNa [54]. The highly accurate (an accuracy of 0.0005 $cm^{-1}$) set of $H_2^{32}S$ transitions recorded using a FT spectrometer between 2200–4250 $cm^{-1}$ was provided by Horneman (18Horneman [49]) and assigned using the energy levels reported in 98BrCrCrNa [48].

### 3.3. Sources from the HITRAN database

$H_2^{32}S$ has been included in the HITRAN database [85–90] since 1991 [87]. The following are sources for the line positions and energy levels of the $H_2^{32}S$ data in the HITRAN database, up to the 2016 release: 96UlMaKoAl [47], 83FlCaJo [43], 98BrCrCrNa [48], 13AzYuTeMa [42], 94YaKl [40], 95BeYaWiPo [35], 05UlLiBeGr [53], 04UlLiBeGr [58], 03DiNaHuZh [61], 01NaCa_b [66], 84LeFlCaJo [50], 82LaEdGiBo [45], 85LaEdGiBo [80], 94ByNaSmSi [81]. The variational ExoMol AYT2 linelist [91] was used to assign transitions in the $\nu_2$ excited vibrational state in the 2012 release [85].

## 4. Results

The Marvel website (http://www.kkrk.chem.elte.hu/marvelonline) has a version of Marvel which can be run online. The variable NQN (number of quantum numbers) is 7 in the case of hydrogen sulfide, as illustrated in Table 3 which shows an extract of the *ortho* input file to Marvel.

Marvel automatically assigns the lowest energy state in a particular component of the spectroscopic network to 0. The ground rovibrational state is included in the *para* set of energy levels, however there needs to be a "magic number", corresponding to the energy of the lowest *ortho* state, which is added to all the Marvel *ortho*-symmetry energies. Here, this was taken as the ground vibrational state $(\nu_1,\ \nu_2,\ \nu_3) = (0,\ 0,\ 0)$ with the lowest rotational energy (see Section 2.2), $J = 1, K_a = 0, K_c = 1,$ of 94KoJe [78], who determined the value of 13.74631 $cm^{-1}$. The output for the *ortho* energies in the supplementary data, and the extract in Table 6, all have this magic number added for the ortho principal spectroscopic network. There are a small number (4 *para*) of energy levels which are not joined to either of the principal components. If more experimental transitions became available in the future it would be possible to link these to the para principal network.

We collated and considered a total of 44 325 transitions from 33 experimental sources (25 474 *ortho* and 18 851 *para*). Of those 254 were found to be inconsistent (could not be validated to within 0.035 $cm^{-1}$) with others and so removed from the final data set, leaving a total of 44 071 transitions used as input into Marvel (25 293 *ortho* and 18 778 *para*).

Fig. 1 gives a visual representation of NumTrans, the number of transitions which link the states of the Marvel *ortho*-$H_2^{32}S$ network, against corresponding upper state energies. Those upper states which are dark blue in colour, linked by only 1 transition, should be considered less reliable than those in red, which are supported by hundreds of different transitions, up to 404. The values of NumTrans for each level are given in the energy level files in the supplementary data.

## 5. Comparison to other derived energy levels

We used a number of sources to compare energy level values against those determined in this work. 94KoJe [78] contains a list of energy levels, which are taken or calculated from other sources [31,43,50,76,80,84]; see Table 7 for a breakdown by vibrational band. AYT2 [91] is a theoretical variational linelist for $H_2{}^{32}S$ calculated as part of the ExoMol project [92,93], a database of theoretical linelists for molecules of astrophysical importance. AYT2 is appropriate up to temperatures of around 2000 K and designed for use in characterising the atmospheres of cool stars and exoplanets. The states file, available from https://www.exomol.com,

**Table 6**
Extract from the MARVEL output file for the *ortho* energy levels of $H_2^{32}S$. The full file is supplied as part of the supplementary information to this paper. All energies and uncertainties are in units of $cm^{-1}$. NumTrans gives the number of transitions which are linked to that particular energy level. Assignments are as given by Table 1.

| Assignment | | | | | | | Energy | Uncertainty | NumTrans | Sym |
|---|---|---|---|---|---|---|---|---|---|---|
| 0 | 0 | 0 | 1 | 0 | 1 | ortho | 13.746310 | 0.000001 | 177 | B1 |
| 0 | 0 | 0 | 1 | 1 | 0 | ortho | 19.375630 | 0.000001 | 153 | B2 |
| 0 | 0 | 0 | 2 | 1 | 2 | ortho | 38.297765 | 0.000002 | 271 | B2 |
| 0 | 0 | 0 | 2 | 2 | 1 | ortho | 55.161605 | 0.000002 | 265 | B1 |
| 0 | 0 | 0 | 3 | 0 | 3 | ortho | 71.424233 | 0.000002 | 282 | B1 |
| 0 | 0 | 0 | 3 | 1 | 2 | ortho | 95.056325 | 0.000001 | 344 | B2 |
| 0 | 0 | 0 | 3 | 2 | 1 | ortho | 107.368228 | 0.000001 | 331 | B1 |
| 0 | 0 | 0 | 4 | 1 | 4 | ortho | 114.177613 | 0.000001 | 282 | B2 |
| 0 | 0 | 0 | 3 | 3 | 0 | ortho | 117.392015 | 0.000001 | 265 | B2 |
| 0 | 0 | 0 | 4 | 2 | 3 | ortho | 148.418340 | 0.000001 | 379 | B1 |

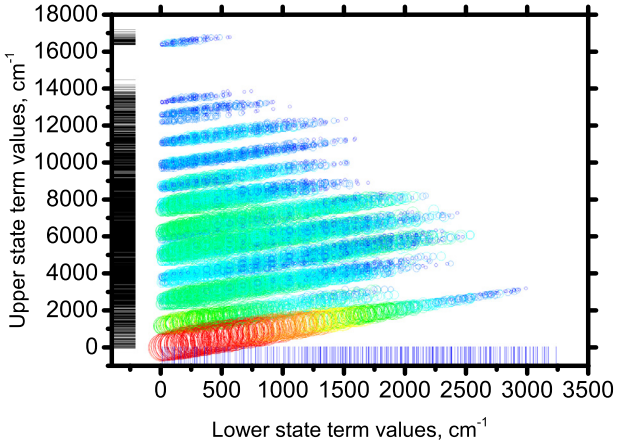


**Fig. 1.** The lower-state energies of the experimental *ortho*-$H_2^{32}S$ transitions used in this work, against corresponding upper-state energies. The vertical bars along the horizontal-axis show the lower-state energies, while the horizontal bars along the vertical-axis give the upper-state energies. Each circle represents a particular transition, with the size proportional to the log of NumTrans, the number of transitions supporting the upper state. This value ranges from 1 (dark blue) to 404 (red). (For interpretation of the references to colour in this figure legend, the reader is referred to the web version of this article.)

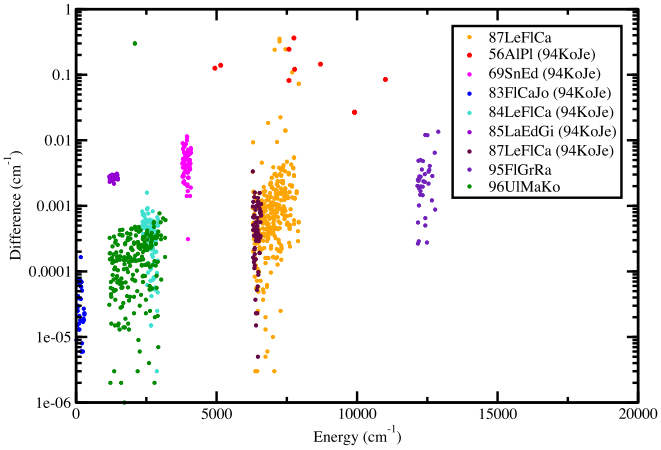


**Fig. 2.** Deviations in $cm^{-1}$ between energy levels from this work and: 94KoJe [78] (see Table 7), 95FlGrRaSt [79], 87LeFlCaAr [76], 96UlMaKoAl [47]. Note the logarithmic vertical–axis.

gives the calculated energy levels, which can be compared against our empirical energy levels. For more information on the format of the ExoMol data files, please refer to [93]. 95FlGrRaSt [79] contains rovibrational energy levels from the $(v_1, v_2, v_3) = (2, 0, 3)$ and (3,0,2) vibrational bands. The authors outline an experimental procedure used to deduce these levels but they do not provide the experimental transition data so we could not include the data from this source in our dataset. 87LeFlCaAr [76] has a table of rovibrational energy levels for the $(v_1, v_2, v_3) = (2, 1, 0)$, (1, 1, 1) and (0, 1, 2) vibrational bands. 96UlMaKoAl [47] contains rovibrational energy levels from the $(v_1, v_2, v_3) = (0, 1, 0)$ vibrational band.

We compared the pure rotational levels determined in this work both against those given in 94KoJe [78] and the calculated values from the AYT2 linelist [91], up to $J = 5$. These data are given in Table 8. The pure rotational levels are closer to those from the experimentally determined sources of 94KoJe than to those of variationally calculated AYT2, as would be expected.

The pure vibrational levels from this work are also compared with those from 94KoJe [78] and AYT2 [91], see Table 9. It should be noted here that there are some differences in labelling between these data sources and those used in this work. For example, the pure vibrational levels of 94KoJe [78] which are labelled $(v_1, v_2, v_3) = (2, 0, 2)$, (1, 0, 2) and (3, 0, 0), match the normal mode labelling of (4, 0, 0), (3, 0, 0) and (1, 0, 2), respectively, according to the labelling of 01TyTaSc [82] and the experimental sources used in this work.

We compared all the rovibrational energy levels given in 94KoJe [78], 95FlGrRaSt [79], 96UlMaKoAl [47], and 87LeFlCaAr [76] against our set of MARVEL energy levels, taking the aforementioned labelling differences into account for 94KoJe [78] (see Table 7). These comparisons are illustrated in Fig. 2. Most levels are in good agreement, with only a few levels with differences between 0.1–0.4 $cm^{-1}$. These levels with the largest differences are from 87LeFlCaAr [76] and 56AlPl [31]. All the levels which are compared to those of 87LeFlCaAr [76] have several transitions which link them to other energy levels in our MARVEL dataset, and originate from different sources, which increases their reliability. This indicates that the lack of accuracy for these particular energies originates from 87LeFlCaAr [76] and not the MARVEL dataset. The transition data from 56AlPl [31] was considered for use in the current study, but the data could not be validated with that from newer sources (see Table 5), and so the energy levels are also assumed to be unreliable.

As mentioned above, AYT2 [91] is a theoretical variational linelist for $H_2^{32}S$ calculated as part of the ExoMol project [92,93]. Highly accurate experimental energy levels provide essential input for testing and improving theoretically calculated line positions such as those within AYT2. The ExoMol data format convention is to have a 'states' and a 'trans' file. The states file gives the calculated rovibrational energy levels, which can be compared against our empirical energy levels, and the trans file contains the Einstein–*A* coefficients for transitions between these states [93].

**Table 7**
Original sources of energy level data from 94KoJe [78].

| Tag | Ref. | Vibrational bands | Comments |
|---|---|---|---|
| 83FlCaJo | [43] | (0, 0, 0) | Experimental source used in this work |
| 85LaEdGiBo | [80] | (0, 1, 0) | Calculated values, compared to experimental values from 83FlCaJo [43] |
| 84LeFlCaJo | [50] | (0, 2, 0) (1, 0, 0) (0, 0, 1) | Experimental source used in this work |
| 69SnEd | [84] | (1, 1, 0) (0, 1, 1) | Experimental source used in this work |
| 56AlPl | [31] | (0, 2, 1) (2, 0, 0) (1, 0, 1) (3, 0, 0) (2, 0, 1) (1, 0, 2) (0, 0, 3) (2, 1, 1) (3, 0, 1) (2, 0, 2) (1, 0, 3) (3, 1, 1) | Data source not considered reliable. All $J = 0$ levels only. |
| 87LeFlCaAr | [76] | (2, 1, 0) (1, 1, 1) | 94KoJe [78] only contains levels from this source up to $J = 5$. See text and Fig. 2 for a full comparison. |

**Table 8**
Comparison of pure rotational levels from this work with those of 94KoJe [78] (see Table 7) and AYT2 [91] up to $J = 5$. NumTrans gives the number of transitions linking a particular state. All energies and uncertainties are in $cm^{-1}$. The uncertainty refers to this work.

| $J$ $K_a$ $K_c$ | State | Sym | NumTrans | Uncertainty | This work | 94KoJe | Difference | AYT2 | Difference |
|---|---|---|---|---|---|---|---|---|---|
| 0 0 0 | *para* | $A_1$ | 58 | 0.000098 | 0 | 0 | 0 | 0 | 0 |
| 1 0 1 | *ortho* | $B_1$ | 170 | 0.000001 | 13.746310 | 13.74631 | 0.00000 | 13.746340 | 0.000030 |
| 1 1 1 | *para* | $A_2$ | 157 | 0.000002 | 15.090119 | 15.09011 | -0.00001 | 15.090151 | 0.000032 |
| 1 1 0 | *ortho* | $B_2$ | 147 | 0.000001 | 19.375630 | 19.37563 | 0.00000 | 19.375563 | -0.000067 |
| 2 0 2 | *para* | $A_1$ | 223 | 0.000001 | 38.016095 | 38.01607 | -0.00003 | 38.016264 | 0.000169 |
| 2 1 2 | *ortho* | $B_2$ | 258 | 0.000002 | 38.297765 | 38.29775 | -0.00001 | 38.297961 | 0.000196 |
| 2 1 1 | *para* | $A_2$ | 211 | 0.000001 | 51.140188 | 51.14016 | -0.00003 | 51.140060 | -0.000128 |
| 2 2 1 | *ortho* | $B_1$ | 253 | 0.000002 | 55.161605 | 55.16158 | -0.00003 | 55.161460 | -0.000145 |
| 2 2 0 | *para* | $A_1$ | 181 | 0.000001 | 58.368870 | 58.36884 | -0.00003 | 58.368621 | -0.000249 |
| 3 0 3 | *ortho* | $B_1$ | 265 | 0.000002 | 71.424221 | 71.42426 | 0.00004 | 71.424760 | 0.000539 |
| 3 1 3 | *para* | $A_2$ | 213 | 0.000001 | 71.465192 | 71.46515 | -0.00004 | 71.465653 | 0.000461 |
| 3 1 2 | *ortho* | $B_2$ | 329 | 0.000001 | 95.056313 | 95.05630 | -0.00001 | 95.056267 | -0.000046 |
| 3 2 2 | *para* | $A_1$ | 272 | 0.000001 | 96.392529 | 96.39246 | -0.00007 | 96.392428 | -0.000101 |
| 3 2 1 | *ortho* | $B_1$ | 313 | 0.000001 | 107.368216 | 107.36820 | -0.00002 | 107.367927 | -0.000289 |
| 4 0 4 | *para* | $A_1$ | 205 | 0.000001 | 114.172246 | 114.17217 | -0.00008 | 114.173085 | 0.000839 |
| 4 1 4 | *ortho* | $B_2$ | 270 | 0.000001 | 114.177601 | 114.17758 | -0.00002 | 114.178495 | 0.000894 |
| 3 3 1 | *para* | $A_2$ | 250 | 0.000002 | 115.340656 | 115.34059 | -0.00007 | 115.340038 | -0.000618 |
| 3 3 0 | *ortho* | $B_2$ | 247 | 0.000001 | 117.392003 | 117.39199 | -0.00001 | 117.391407 | -0.000596 |
| 4 1 3 | *para* | $A_2$ | 306 | 0.000001 | 148.140653 | 148.14058 | -0.00007 | 148.140740 | 0.000087 |
| 4 2 3 | *ortho* | $B_1$ | 362 | 0.000001 | 148.418328 | 148.41831 | -0.00002 | 148.418470 | 0.000142 |
| 5 0 5 | *ortho* | $B_1$ | 264 | 0.000045 | 166.343488 | 166.34345 | -0.00004 | 166.344887 | 0.001399 |
| 5 1 5 | *para* | $A_2$ | 196 | 0.000077 | 166.344005 | 166.34417 | 0.00016 | 166.345606 | 0.001601 |
| 4 2 2 | *para* | $A_1$ | 308 | 0.000001 | 170.335799 | 170.33574 | -0.00006 | 170.335471 | -0.000328 |
| 4 3 2 | *ortho* | $B_2$ | 383 | 0.000002 | 173.967266 | 173.96726 | -0.00001 | 173.966794 | -0.000472 |
| 4 3 1 | *para* | $A_2$ | 261 | 0.000001 | 182.648548 | 182.64849 | -0.00006 | 182.647978 | -0.000570 |
| 4 4 1 | *ortho* | $B_1$ | 290 | 0.000002 | 195.661414 | 195.66142 | 0.00001 | 195.659965 | -0.001449 |
| 4 4 0 | *para* | $A_1$ | 219 | 0.000003 | 196.802189 | 196.80212 | -0.00007 | 196.800713 | -0.001476 |
| 5 1 4 | *ortho* | $B_2$ | 356 | 0.000037 | 210.217262 | 210.21727 | 0.00001 | 210.217731 | 0.000469 |
| 5 2 4 | *para* | $A_1$ | 270 | 0.000001 | 210.264821 | 210.26477 | -0.00005 | 210.265229 | 0.000408 |
| 5 2 3 | *ortho* | $B_1$ | 387 | 0.000001 | 243.343434 | 243.34344 | 0.00001 | 243.343211 | -0.000223 |
| 5 3 3 | *para* | $A_2$ | 333 | 0.000001 | 244.392517 | 244.39250 | -0.00002 | 244.392149 | -0.000368 |
| 5 3 2 | *ortho* | $B_2$ | 363 | 0.000001 | 263.738931 | 263.73895 | 0.00002 | 263.738560 | -0.000371 |
| 5 4 2 | *para* | $A_1$ | 298 | 0.000001 | 271.106067 | 271.10604 | -0.00003 | 271.104809 | -0.001258 |
| 5 4 1 | *ortho* | $B_1$ | 316 | 0.000002 | 277.337562 | 277.33758 | 0.00002 | 277.336633 | -0.000929 |
| 5 5 1 | *para* | $A_2$ | 229 | 0.000002 | 296.104442 | 296.10442 | -0.00002 | 296.101282 | -0.003160 |
| 5 5 0 | *ortho* | $B_2$ | 278 | 0.000001 | 296.677577 | 296.67760 | 0.00002 | 296.674560 | -0.003017 |

This format allows calculated linelists to be retrospectively updated using more reliable experimental energy levels in order to improve their accuracy, see [94] for an example.

To compare our energy levels with those from the AYT2 [91] linelist, a comparable states file was made; we labelled our states with the same $A_1$, $A_2$, $B_1$, $B_2$ symmetry labels which are given in the AYT2 states file, see Table 2. We then matched all states with this same symmetry, $\nu_2$, $\nu_1 + \nu_3$, and $J$, and searched for the closest value within these given parameters. Fig. 3 gives the result of this comparison.

Work is underway to update the existing ExoMol AYT2 states file and linelist based on the energy levels obtained in this work, using only those levels based on the transitions we are most sure about. Care should be taken in general when using MARVEL energy levels with a low value of NumTrans (see Fig. 1). This, along with the uncertainty, gives an indication of the reliability of a particular energy level.

## 6. Conclusions

A total of 44 325 measured experimental rovibrational transitions of $H_2^{32}S$ from 33 publications have been considered in this work. From this set, 3969 *ortho*- and 3467 *para*-$H_2^{32}S$ energy levels have been determined using the Measured Active Rotational-Vibrational Energy Levels (MARVEL) technique. These results have been carefully compared with alternative compilations of energy levels.

A variational high-temperature linelist for $H_2^{32}S$ has been computed as part of the ExoMol project, AYT2 [91]. Our new MARVEL energy levels will be used to improve the accuracy of this theoretical linelist.

A significant part of this work was performed by pupils from Highams Park School in London, as part of a project known as ORBYTS (Original Research By Young Twinkle Students) [95]. The MARVEL studies of $^{12}C_2H_2$ [26] and $^{48}Ti^{16}O$ [18] were also per-

**Table 9**
Comparison of pure vibrational levels ($J = 0$) from this work with those of 94KoJe [78] (see Table 7) and AYT2 [91]. NT stands for NumTrans, the number of transitions linking a particular state. All energies and uncertainties are in $cm^{-1}$. The uncertainty refers to this work. State is from this work and Sym is the corresponding symmetry label as used in AYT2 [91] (see Section 2.2).

| $\nu_1$ $\nu_2$ $\nu_3$ | State | Sym | NT | Uncertainty | This work | 94KoJe | Difference | AYT2 | Difference |
|---|---|---|---|---|---|---|---|---|---|
| 0 0 0 | *para* | $A_1$ | 58 | 0.000098 | 0 | | | 0 | 0 |
| 0 1 0 | *para* | $A_1$ | 5 | 0.000477 | 1182.576991 | 1182.5742 | -0.0028 | 1182.569618 | -0.007373 |
| 0 2 0 | *para* | $A_1$ | 4 | 0.000629 | 2353.964679 | 2353.9655 | 0.0008 | 2353.907317 | -0.057362 |
| 1 0 0 | *para* | $A_1$ | 3 | 0.000663 | 2614.407743 | 2614.4074 | -0.0003 | 2614.394829 | -0.012914 |
| 0 0 1 | *ortho* | $B_2$ | 2 | 0.000669 | 2628.454821 | 2628.4552 | 0.0004 | 2628.463320 | 0.008499 |
| 0 3 0 | *para* | $A_1$ | 3 | 0.000621 | 3513.789974 | | | 3513.705072 | -0.084902 |
| 1 1 0 | *para* | $A_1$ | 3 | 0.000390 | 3779.166566 | 3779.1710 | 0.0044 | 3779.189348 | 0.022782 |
| 0 1 1 | *ortho* | $B_2$ | 2 | 0.000625 | 3789.269211 | 3789.2720 | 0.0028 | 3789.269878 | 0.000667 |
| 0 4 0 | *para* | $A_1$ | 1 | 0.001000 | 4661.672219 | | | 4661.605794 | -0.066425 |
| 1 2 0 | *para* | $A_1$ | 2 | 0.000707 | 4932.699369 | | | 4932.688937 | -0.010432 |
| 0 2 1 | *ortho* | $B_2$ | 2 | 0.000707 | 4939.104010 | 4939.2300 | 0.1260 | 4939.129851 | 0.025841 |
| 2 0 0 | *para* | $A_1$ | 2 | 0.000707 | 5144.986319 | 5145.1200 | 0.1337 | 5145.031868 | 0.045549 |
| 1 0 1 | *ortho* | $B_2$ | 2 | 0.000707 | 5147.220560 | 5147.3600 | 0.1394 | 5147.166622 | -0.053938 |
| 0 0 2 | *para* | $A_1$ | 2 | 0.000707 | 5243.101919 | | | 5243.158956 | 0.057037 |
| 1 3 0 | *para* | $A_1$ | 2 | 0.000928 | 6074.581067 | | | 6074.566059 | -0.015008 |
| 0 3 1 | *ortho* | $B_2$ | 2 | 0.000707 | 6077.594560 | | | 6077.626636 | 0.032076 |
| 2 1 0 | *para* | $A_1$ | 2 | 0.000707 | 6288.146119 | 6288.1428 | -0.0033 | 6288.134723 | -0.011396 |
| 1 1 1 | *ortho* | $B_2$ | 3 | 0.000637 | 6289.172875 | 6289.1739 | 0.0010 | 6289.128284 | -0.044591 |
| 1 2 1 | *ortho* | $B_2$ | 4 | 0.000632 | 7420.092707 | | | 7420.077786 | -0.014921 |
| 1 0 2 | *para* | $A_1$ | 1 | 0.002000 | 7576.381719 | 7576.3000 | -0.0817 | 7576.413281 | 0.031562 |
| 2 0 1 | *ortho* | $B_2$ | 2 | 0.001414 | 7576.544710 | 7576.3000 | -0.2447 | 7576.596211 | 0.051501 |
| 3 0 0 | *para* | $A_1$ | 2 | 0.001414 | 7752.263219 | 7751.9000 | -0.3632 | 7752.343205 | 0.079986 |
| 0 0 3 | *ortho* | $B_2$ | 2 | 0.001414 | 7779.321260 | 7779.2000 | -0.1213 | 7779.352004 | 0.030744 |
| 1 3 1 | *ortho* | $B_2$ | 1 | 0.002000 | 8539.561310 | | | 8539.565999 | 0.004689 |
| 1 1 2 | *para* | $A_1$ | 2 | 0.001414 | 8697.141469 | | | 8697.133905 | -0.007564 |
| 2 1 1 | *ortho* | $B_2$ | 2 | 0.001481 | 8697.154984 | 8697.3000 | 0.1450 | 8697.179341 | 0.024357 |
| 1 4 1 | *ortho* | $B_2$ | 1 | 0.005000 | 9647.167310 | | | 9647.098855 | -0.068455 |
| 2 2 1 | *ortho* | $B_2$ | 1 | 0.005000 | 9806.667310 | | | 9806.712978 | 0.045668 |
| 1 2 2 | *para* | $A_1$ | 1 | 0.005000 | 9806.733119 | | | 9806.748170 | 0.015051 |
| 2 0 2 | *para* | $B_2$ | 1 | 0.005000 | 9911.023119 | 9911.0500 | 0.0269 | 9911.102285 | 0.079166 |
| 3 0 1 | *ortho* | $A_1$ | 1 | 0.005000 | 9911.023310 | 9911.0500 | 0.0267 | 9911.112478 | 0.089168 |
| 3 1 1 | *ortho* | $A_1$ | 1 | 0.005000 | 11008.695310 | 11008.7800 | 0.0847 | 11008.774494 | 0.079184 |
| 3 0 2 | *para* | $A_1$ | 1 | 0.001000 | 12149.460119 | | | 12149.552318 | 0.092199 |
| 1 0 4 | *para* | $A_1$ | 1 | 0.015000 | 12524.637119 | | | 12524.834491 | 0.197372 |
| 4 0 1 | *ortho* | $B_2$ | 1 | 0.015000 | 12525.214310 | | | 12525.346292 | 0.131982 |
| 3 1 2 | *para* | $B_2$ | 1 | 0.015000 | 13222.762119 | | | 13222.790827 | 0.028708 |
| 2 1 3 | *ortho* | $A_1$ | 1 | 0.015000 | 13222.772310 | | | 13222.798559 | 0.026249 |

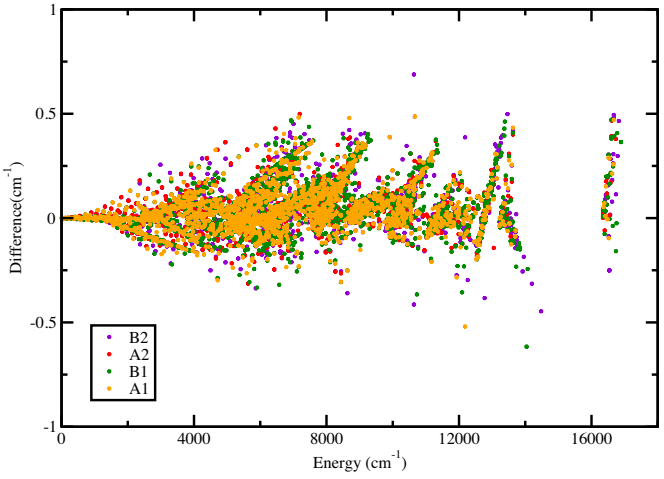


**Fig. 3.** Deviations, in $cm^{-1}$, between the MARVEL energy levels from this work and the variationally calculated linelist AYT2 [91]. Different colors represent different rovibrational symmetries (see Table 2 in Section 2.2).

formed as part of the ORBYTS project and further studies on other key molecules will be published in due course, involving high-school students from the UK, Australia, and Hungary. A paper discussing our experiences of performing original research in collaboration with school children can be found elsewhere [96].

## Acknowledgements

We would like to thank Jon Barker, Fawad Sheikh, and Sheila Smith from Highams Park School for continued support and enthusiasm, along with Highams Park students Jack Franklin and Samuel Sheppard for their assistance in this project. We are grateful to Laura McKemmish for helpful discussions and advice, Clara Sousa-Silva for setting up the ORBYTS education project, and to Anita Heward, Will Dunn, Marcell Tessenyi, and the rest of the Twinkle team for their ongoing support. We give thanks to Shuiming Hu for contributions to the data used in this work. This work was supported by STFC Project ST/J002925, the RSF (grant 17-12-01204), the ERC under Advanced Investigator Project 267219, NKFIH (grant K119658), and the COST action MOLIM: Molecules in Motion (CM1405).

## Supplementary material

Supplementary material associated with this article can be found, in the online version, at doi:10.1016/j.jqsrt.2018.07.012.

## References

[1] Salama F, Allamandola L, Witteborn F, Cruikshank D, Sandford S, Bregman J. The 2.5–5.0 μm spectra of Io: Evidence for $H_2S$ and $H_2O$ frozen in $SO_2$. Icarus 1990;83:66–82. doi:10.1016/0019-1035(90)90006-U.
[2] Schulze-Makuch D, Grinspoon DH, Abbas O, Irwin LN, Bullock MA. A sulfur-based survival strategy for putative phototrophic life in the Venusian atmosphere. Astrobiology 2004;4:11–18. doi:10.1089/153110704773600203.

[3] Tennyson J, Yurchenko SN. Laboratory spectra of hot molecules: data needs for hot super-earth exoplanets. Mol Astrophys 2017;8:1–18. doi:10.1016/j.molap.2017.05.002.

[4] Irwin PGJ, Toledo D, Garland R, Teanby NA, Fletcher LN, Orton GA, Bezard B. Detection of hydrogen sulfide above the clouds in Uranus's atmosphere. Nat Astron 2018;2:420–7. doi:10.1038/s41550-018-0432-1.

[5] Pace NR. A molecular view of microbial diversity and the biosphere. Science 1997;276(5313):734–40. doi:10.1126/science.276.5313.734.

[6] Kaltenegger L, Sasselov D. Detecting planetary geochemical cycles on exoplanets: Atmospheric signatures and the case of $SO_2$. Astrophys J 2010;708:1162. doi:10.1088/0004-637X/708/2/1162.

[7] King SB. Potential biological chemistry of hydrogen sulfide ($H_2S$) with the nitrogen oxides. Free Radical Biol Med 2013;55(Supplement C):1–7. doi:10.1016/j.freeradbiomed.2012.11.005.

[8] Bazhanov N, Ansar M, Ivanciuc T, Garofalo RP, Casola A. Hydrogen sulfide: a novel player in airway development, pathophysiology of respiratory diseases, and antiviral defenses. Am J Respiratory Cell Molec Bio 2017;57:403–10. doi:10.1165/rcmb.2017-0114TR.

[9] Ciaffoni L, Cummings BL, Denzer W, Peverall R, Procter SR, Ritchie GAD. Line strength and collisional broadening studies of hydrogen sulphide in the 1.58 μm region using diode laser spectroscopy. Appl Phys B 2008;92:627. doi:10.1007/s00340-008-3119-y.

[10] Thaddeus P, Kutner ML, Penzias AA, Wilson RW, Jefferts KB. Interstellar hydrogen sulfide. Astron Astrophys 1972;176:73. doi:10.1086/181023.

[11] Furtenbacher T, Császár AG, Tennyson J. MARVEL: measured active rotational-vibrational energy levels. J Mol Spectrosc 2007;245:115–25. doi:10.1016/j.jms.2007.07.005.

[12] Furtenbacher T, Császár AG. The role of intensities in determining characteristics of spectroscopic networks. J Molec Struct (THEOCHEM) 2012;1009:123–9. doi:10.1016/j.molstruc.2011.10.057.

[13] Furtenbacher T, Császár AG. MARVEL: measured active rotational-vibrational energy levels. II. algorithmic improvements. J Quant Spectrosc Radiat Transf 2012;113:929–35. doi:10.1016/j.jqsrt.2012.01.005.

[14] Polovtseva ER, Lavrentiev NA, Voronina SS, Naumenko OV, Fazliev AZ. Information system for molecular spectroscopy. 5. Ro-vibrational transitions and energy levels of the hydrogen sulfide molecule. Atmos Oceanic Optics 2012;25:157–65. doi:10.1134/S1024856012020133.

[15] Császár AG, Furtenbacher T. Spectroscopic networks. J Mol Spectrosc 2011;266:99–103. doi:10.1016/j.jms.2011.03.031.

[16] Árendás P, Furtenbacher T, Császár AG. On spectra of spectra. J Math Chem 2016;54:806–22. doi:10.1007/s10910-016-0591-1.

[17] Furtenbacher T, Szabó I, Császár AG, Bernath PF, Yurchenko SN, Tennyson J. Experimental energy levels and partition function of the $^{12}C_2$ molecule. Astrophys J Suppl 2016;224:44. doi:10.3847/0067-0049/224/2/44.

[18] McKemmish LK, Masseron T, Sheppard S, Sandeman E, Schofield Z, Furtenbacher T, Császár AG, Tennyson J, Sousa-Silva C. MARVEL Analysis of the measured high-resolution spectra of $^{48}Ti^{16}O$. Astrophys J Suppl 2017;228:15. doi:10.3847/1538-4365/228/2/15.

[19] Tennyson J, Bernath PF, Brown LR, Campargue A, Carleer MR, Császár AG, Gamache RR, Hodges JT, Jenouvrier A, Naumenko OV, Polyansky OL, Rothman LS, Toth RA, Vandaele AC, Zobov NF, Daumont L, Fazliev AZ, Furtenbacher T, Gordon IE, Mikhailenko SN, Shirin SV. IUPAC critical evaluation of the rotational-vibrational spectra of water vapor. Part I. Energy levels and transition wavenumbers for $H_2^{17}O$ and $H_2^{18}O$. J Quant Spectrosc Radiat Transf 2009;110:573–96. doi:10.1016/j.jqsrt.2009.02.014.

[20] Tennyson J, Bernath PF, Brown LR, Campargue A, Carleer MR, Császár AG, Daumont L, Gamache RR, Hodges JT, Naumenko OV, Polyansky OL, Rothman LS, Toth RA, Vandaele AC, Zobov NF, Fazliev AZ, Furtenbacher T, Gordon IE, Mikhailenko SN, Voronin BA. IUPAC critical evaluation of the rotational-vibrational spectra of water vapor. Part II. Energy levels and transition wavenumbers for $HD^{16}O$, $HD^{17}O$, and $HD^{18}O$. J Quant Spectrosc Radiat Transf 2010;111:2160–84. doi:10.1016/j.jqsrt.2010.06.012.

[21] Tennyson J, Bernath PF, Brown LR, Campargue A, Carleer MR, Császár AG, Daumont L, Gamache RR, Hodges JT, Naumenko OV, Polyansky OL, Rothmam LS, Vandaele AC, Zobov NF, Al Derzi AR, Fábri C, Fazliev AZ, Furtenbacher T, Gordon IE, Lodi L, Mizus II. IUPAC critical evaluation of the rotational-vibrational spectra of water vapor. Part III. Energy levels and transition wavenumbers for $H_2^{16}O$. J Quant Spectrosc Radiat Transf 2013;117:29–80. doi:10.1016/j.jqsrt.2012.10.002.

[22] Tennyson J, Bernath PF, Brown LR, Campargue A, Császár AG, Daumont L, Gamache RR, Hodges JT, Naumenko OV, Polyansky OL, Rothmam LS, Vandaele AC, Zobov NF, Dénes N, Fazliev AZ, Furtenbacher T, Gordon IE, Hu SM, Szidarovszky T, Vasilenko IA. IUPAC critical evaluation of the rotational-vibrational spectra of water vapor. Part IV. Energy levels and transition wavenumbers for $D_2^{16}O$, $D_2^{17}O$ and $D_2^{18}O$. J Quant Spectrosc Radiat Transf 2014;142:93–108. doi:10.1016/j.jqsrt.2014.03.019.

[23] Furtenbacher T., Tennyson J., Naumenko O.V., Polyansky O.L., Zobov N.F., Császár A.G.. The 2018 update of the IUPAC database of water energy levels. J Quant Spectrosc Radiat Transf (In preparation).

[24] Furtenbacher T, Szidarovszky T, Mátyus E, Fábri C, Császár AG. Analysis of the rotational–vibrational states of the molecular ion $H_3^+$. J Chem Theory Comput 2013;9:5471–8. doi:10.1021/ct4004355.

[25] Furtenbacher T, Szidarovszky T, Fábri C, Császár AG. MARVEL analysis of the rotational–vibrational states of the molecular ions $H_2D^+$ and $D_2H^+$. Phys Chem Chem Phys 2013;15:10181–93. doi:10.1039/c3cp44610g.

[26] Chubb KL, Joseph M, Franklin J, Choudhury N, Furtenbacher T, Császár AG, Gaspard G, Oguoko P, Kelly A, Yurchenko SN, Tennyson J, Sousa-Silva C. MARVEL analysis of the measured high-resolution spectra of $C_2H_2$. J Quant Spectrosc Radiat Transf 2018;204:42–55. doi:10.1016/j.jqsrt.2017.08.018.

[27] Al Derzi AR, Furtenbacher T, Yurchenko SN, Tennyson J, Császár AG. MARVEL analysis of the measured high-resolution spectra of $^{14}NH_3$. J Quant Spectrosc Radiat Transf 2015;161:117–30. doi:10.1016/j.jqsrt.2015.03.034.

[28] Furtenbacher T., Coles P.A., Tennyson J., Császár A.G.. Updated MARVEL energy levels for ammonia. J Quant Spectrosc Radiat Transf;To be submitted.

[29] Fábri C, Mátyus E, Furtenbacher T, Nemes L, Mihály B, Zoltáni T, Császár AG. Variational quantum mechanical and active database approaches to the rotational-vibrational spectroscopy of ketene, $H_2CCO$. J Chem Phys 2011;135:094307.

[30] Herman M, Lievin J. Acetylene- from intensity alternation in spectra to ortho and para molecule. J Chem Educ 1982;59:17. doi:10.1021/ed059p17.

[31] Allen Jr HC, Plyler EK. Infrared spectrum of hydrogen sulfide. J Chem Phys 1956;25:1132–6. doi:10.1063/1.1743164.

[32] Bunker PR, Jensen P. Molecular Symmetry and Spectroscopy. 2nd ed. Ottawa: NRC Research Press; 1998.

[33] Miani A, Tennyson J. Can ortho-para transitions for water be observed? J Chem Phys 2004;120:2732–9.

[34] Helminger P, Cook RL, De Lucia FC. Microwave spectrum and centrifugal distortion effects of $H_2S$. J Chem Phys 1972;56:4581–4. doi:10.1063/1.1677906.

[35] Belov SP, Yamada KMT, Winnewisser G, Poteau L, Bocquet R, Demaison J, Polyansky O, Tretyakov MY. Terahertz rotational spectrum of $H_2S$. J Mol Spectrosc 1995;173:380–90. doi:10.1006/jmsp.1995.1242.

[36] Cupp RE, Keikpf RA, Gallagher JJ. Hyperfine structure in the millimeter spectrum of hydrogen sulfide electric spectroscopy on asymmetric-top molecules. Phys Rev 1968;171:60–9. doi:10.1103/PhysRev.171.60.

[37] Huiszoon C. A high resolution spectrometer for the shorter millimeter wavelength region. Rev Sci Instrum 1971;42:477–81. doi:10.1063/1.1685135.

[38] Cazzoli G, Puzzarini C. The rotational spectrum of hydrogen sulfide: The $H_2^{33}S$ and $H_2^{32}S$ isotopologues revisited. J Mol Spectrosc 2014;298(Supplement C):31–7. doi:10.1016/j.jms.2014.02.002.

[39] Burenin AV, Fevralskikh TM, Melnikov AA, Shapin SM. Microwave spectrum of the hydrogen sulfide molecule $H_2^{32}S$ in the ground state. J Mol Spectrosc 1985;109:1–7. doi:10.1016/0022-2852(85)90045-1.

[40] Yamada KMT, Klee S. Pure rotational spectrum of $H_2S$ in the far-infrared region measured by FTIR spectroscopy. J Mol Spectrosc 1994;166:395–405. doi:10.1006/jmsp.1994.1204.

[41] Cazzoli G, Puzzarini C. Sub-doppler resolution in the THz frequency domain: 1\, kHz accuracy at 1 THz by exploiting the lamb-dip technique. J Phys Chem A 2013;117:13759–66. doi:10.1021/jp407980f.

[42] Azzam AAA, Yurchenko SN, Tennyson J, Martin MA, Pirali O. Terahertz spectroscopy of hydrogen sulfide. J Quant Spectrosc Radiat Transf 2013;130:341–51. doi:10.1016/j.jqsrt.2013.05.035.

[43] Flaud JM, Camy-Peyret C, Johns JWC. The far-infrared spectrum of hydrogen-sulfide - the (000) rotational-constants of $H_2^{32}S$, $H_2^{33}S$ and $H_2^{34}S$. Can J Phys 1983;61:1462–73. doi:10.1139/p83-188.

[44] Ulenikov ON, Bekhtereva ES, Gromova OV, Glushkov PA, Scherbakov AP, Horneman VM, Sydow C, Maul C, Bauerecker S. Extended analysis of the high resolution FTIR spectra of $H_2^MS$ (M = 32,33,34,36) in the region of the bending fundamental band: the $\nu_2$ and bands: line positions, strengths, and pressure broadening widths. J Quant Spectrosc Radiat Transf 2018;216:76–98. doi:10.1016/j.jqsrt.2018.05.009.

[45] Lane WC, Edwards TH, Gillis JR, Bonomo FS, Murcray FJ. Analysis of $\nu_2$ of $H_2S$. J Mol Spectrosc 1982;95:365–80. doi:10.1016/0022-2852(82)90136-9.

[46] Strow LL. Measurement and analysis of the $\nu_2$ band of $H_2S$: comparison among several reduced forms of the rotational hamiltonian. J Mol Spectrosc 1983;97:9–28. doi:10.1016/0022-2852(83)90334-X.

[47] Ulenikov ON, Malikova AB, Koivusaari M, Alanko S, Anttila R. High resolution vibrational rotational spectrum of $H_2S$ in the region of the $\nu_2$ fundamental band. J Mol Spectrosc 1996;176:229–35. doi:10.1006/jmsp.1996.0082.

[48] Brown LR, Crisp JA, Crisp D, Naumenko OV, Smirnov MA, Sinitsa LN, Perrin A. The absorption spectrum of $H_2S$ between 2150 and 4260 $cm^{-1}$: Analysis of the positions and intensities in the first ($2\nu_2$, $\nu_1$, and $\nu_3$) and second ($3\nu_2$, $\nu_1/\nu_2$, and $\nu_2/\nu_3$) triad regions. J Mol Spectrosc 1998;188:148–74. doi:10.1006/jmsp.1997.7501.

[49] Horneman VM. Private communication.

[50] Lechuga-Fossat L, Flaud JM, Camy-Peyret C, Johns JWC. The spectrum of natural hydrogen-sulfide between 2150 $cm^{-1}$ and 2950 $cm^{-1}$. Can J Phys 1984;62:1889–923. doi:10.1139/p84-233.

[51] Gillis JR, Edwards TH. Analysis of $2\nu_2$, $\nu_1$, and $\nu_3$ of $H_2S$. J Mol Spectrosc 1981;85:55–73. doi:10.1016/0022-2852(81)90309-X.

[52] Ulenikov ON, Onopenko GA, Koivusaari M, Alanko S, Anttila R. High resolution fourier transform spectrum of $H_2S$ in the 3300–4080 $cm^{-1}$ region. J Mol Spectrosc 1996;176:236–50. doi:10.1006/jmsp.1996.0083.

[53] Ulenikov ON, Liu AW, Bekhtereva ES, Gromova OV, Hao LY, Hu SM. High-resolution fourier transform spectrum of $H_2S$ in the region of the second hexade. J Mol Spectrosc 2005;234:270–8. doi:10.1016/j.jms.2005.09.010.

[54] Brown LR, Crisp JA, Crisp D, Naumenko OV, Smirnov MA, Sinitsa LN. The first hexad of interacting states of $H_2S$ molecule. SPIE 1997;3090:111–13. doi:10.1117/12.267745.

[55] Liu AW. Private communication.

[56] Brown LR, Naumenko OV, Polovtseva ER, Sinitsa LN. Hydrogen sulfide absorption spectrum in the 5700–6600 $cm^{-1}$ spectral region. Proceedings 14th Sym-

posium on High-Resolution Molecular Spectroscopy 2004;5311:59–67. doi:10.1117/12.545192.
[57] Brown LR, Naumenko OV, Polovtseva ER, Sinitsa LN. Absorption spectrum of $H_2S$ between 7200 and 7890 $cm^{-1}$. Proc SPIE 2004;5396:5396–7. doi:10.1117/12.548211.
[58] Ulenikov ON, Liu AW, Bekhtereva ES, Gromova OV, Hao LY, Hu SM. On the study of high-resolution rovibrational spectrum of $H_2S$ in the region of 7300–7900 $cm^{-1}$. J Mol Spectrosc 2004;226:57–70. doi:10.1016/j.jms.2004.03.014.
[59] Ulenikov ON, Liu AW, Bekhtereva ES, Grebneva SV, Deng WP, Gromova OV, Hu SM. High resolution fourier transform spectrum of $H_2S$ in the region of 8500-8900 $cm^{-1}$. J Mol Spectrosc 2004;228:110–19. doi:10.1016/j.jms.2004.07.011.
[60] Brown LR, Naumenko OV, Polovtseva ER, Sinitsa LN. Hydrogen sulfide absorption spectrum in the 8400–8900 $cm^{-1}$ spectral region. Eleventh International Symposium on Atmospheric and Ocean Optics/Atmospheric Physics 2004;5743:1–7. doi:10.1117/12.606253.
[61] Ding Y, Naumenko O, Hu SM, Zhu Q, Bertseva E, Campargue A. The absorption spectrum of $H_2S$ between 9540 and 10 000 $cm^{-1}$ by intracavity laser absorption spectroscopy with a vertical external cavity surface emitting laser. J Mol Spectrosc 2003;217:222–38. doi:10.1016/S0022-2852(02)00037-1.
[62] Naumenko O, Campargue A. $H_2^{32}s$ : First observation of the (70 ±, 0) local mode pair and updated global effective vibrational hamiltonian. J Mol Spectrosc 2001;210:224–32. doi:10.1006/jmsp.2001.8460.
[63] Großkloß R, Rai SB, Stuber R, Demtroder W. Diode laser overtone spectroscopy of hydrogen sulfide. Chem Phys Lett 1994;229:609–15. doi:10.1016/0009-2614(94)01079-X.
[64] Vaittinen O, Biennier L, Campargue A, Flaud JM, Halonen L. Local mode effects on the high-resolution overtone spectrum of $H_2S$ around 12 500 $cm^{-1}$. J Mol Spectrosc 1997;184:288–99. doi:10.1006/jmsp.1997.7319.
[65] Campargue A, Flaud JM. The overtone spectrum of $H_2^{32}S$ near 13 200 $cm^{-1}$. J Mol Spectrosc 1999;194:43–51. doi:10.1006/jmsp.1998.7754.
[66] Naumenko O, Campargue A. Local mode effects in the absorption spectrum of $H_2S$ between 10 780 and 11 330 $cm^{-1}$. J Mol Spectrosc 2001;209:242–53. doi:10.1006/jmsp.2001.8417.
[67] Cours T, Rosmus P, Tyuterev VG. Ab initio dipole moment functions of $H_2^{32}S$ and intensity anomalies in rovibrational spectra. J Chem Phys 2002;117:5192–208. doi:10.1063/1.1499487.
[68] Waschull J, Kuhnemann F, Sumpf B. Self-, air, and helium broadening in the $\nu_2$ band of $H_2S$. J Mol Spectrosc 1994;165:150–8. doi:10.1006/jmsp.1994.1117.
[69] Sumpf B, Meusel I, Kronfeldt HD. Self- and air-broadening in the $\nu_1$ and $\nu_3$ bands of $H_2S$. J Mol Spectrosc 1996;177:143–5. doi:10.1006/jmsp.1996.0126.
[70] Sumpf B, Meusel I, Kronfeldt HD. Noble gas broadening in fundamental bands of $H_2S$. J Mol Spectrosc 1997;184:51–5. doi:10.1006/jmsp.1997.7290.
[71] Sumpf B. Experimental investigation of the self-broadening coefficients in the $\nu_1$ / $\nu_3$ band of $SO_2$ and the $2\nu_2$ band of $H_2S$. J Mol Spectrosc 1997;181:160–7. doi:10.1006/jmsp.1996.7168.
[72] Pickett HM, Poynter RL, Cohen EA, Delitsky ML, Pearson JC, Muller HSP. Submillimeter, millimeter, and microwave spectral line catalog. J Quant Spectrosc Radiat Transf 1998;60:883–90. doi:10.1016/S0022-4073(98)00091-0.
[73] Helminger P, De Lucia FC, Kirchhoff WH. Microwave spectra of molecules of astrophysical interest IV. Hydrogen sulfide. J Phys Chem Ref Data 1973;2:215–23. doi:10.1063/1.3253117.
[74] Kissel A, Sumpf B, Kronfeldt HD, Tikhomirov BA, Ponomarev YN. Molecular-gas-pressure-induced line-shift and line-broadening in the $\nu_2$-band of $H_2S$. J Mol Spectrosc 2002;216:345–54. doi:10.1006/jmsp.2002.8630.
[75] Rothman LS, Rinsland CP, Goldman A, Massie ST, Edwards DP, Flaud JM, Perrin A, Camy-Peyret C, Dana V, Mandin JY, Schroeder J, McCann A, Gamache RR, Wattson R, Yoshino K, Chance KV, Jucks KW, Brown LR, Nemtchinov V, Varanasi P. The HITRAN molecular spectroscopic database and HAWKS (HITRAN atmospheric workstation): 1996 edition. J Quant Spectrosc Radiat Transf 1998;60:665–710. doi:10.1016/S0022-4073(98)00078-8.
[76] Lechuga-Fossat L, Flaud JM, Camy-Peyret C, Arcas P, Cuisenier M. The $H_2S$ spectrum in the 1.6 μm spectral region. Mol Phys 1987;61:23–32. doi:10.1080/00268978700100961.
[77] Azzam AAA. A linelist for the hydrogen sulphide molecule. University College London; 2013. The thesis is available on-line at http://discovery.ucl.ac.uk/1404058/.
[78] Kozin IN, Jensen P. Fourfold clusters of rotational energy levels for $H_2S$ studied with a potential energy surface derived from experiment. J Mol Spectrosc 1994;163:483–509. doi:10.1006/jmsp.1994.1041.
[79] Flaud JM, Grosskloss R, Rai SB, Struber R, Demtroder W, Tate DA, Wang Lg, Gallagher TF. Diode laser spectroscopy of $H_2{}^{32}S$ around 0.82 μm. J Mol Spectrosc 1995;172:275–81. doi:10.1006/jmsp.1995.1175.
[80] Lane WC, Edwards TH, Gillis JR, Bonomo FS, Murcray FJ. Analysis of $\nu_2$ of $H_2^{33}S$ and $H_2^{34}S$. J Mol Spectrosc 1985;111:320–6. doi:10.1016/0022-2852(85)90008-6.
[81] Bykov AD, Naumenko OV, Smirnov MA, Sinitsa LN, Brown LR, Crisp J, Crisp D. The infrared-spectrum of $H_2S$ from 1 to 5 μm. Can J Phys 1994;72:989–1000. doi:10.1139/p94-130.
[82] Tyuterev VG, Tashkun SA, Schwenke DW. An accurate isotopically invariant potential function of the hydrogen sulphide molecule. Chem Phys Lett 2001;348:223–34. doi:10.1016/S0009-2614(01)01093-4.
[83] Miller RE, Leroi GE, Hard TM. Analysis of the pure rotational absorption spectra of hydrogen sulfide and deuterium sulfide. J Chem Phys 1969;50:677–84. doi:10.1063/1.1671116.
[84] Snyder LE, Edwards TH. Simultaneous analysis of the (110) and (011) bands of hydrogen sulfide. J Mol Spectrosc 1969;31:347–61. doi:10.1016/0022-2852(69)90365-8.
[85] Rothman LS, Gordon IE, Babikov Y, Barbe A, Benner DC, Bernath PF, Birk M, Bizzocchi L, Boudon V, Brown LR, Campargue A, Chance K, Cohen EA, Coudert LH, Devi VM, Drouin BJ, Fayt A, Flaud JM, Gamache RR, Harrison JJ, Hartmann JM, Hill C, Hodges JT, Jacquemart D, Jolly A, Lamouroux J, Roy RJL, Li G, Long DA, Lyulin OM, Mackie CJ, Massie ST, Mikhailenko S, Müller HSP, Naumenko OV, Nikitin AV, Orphal J, Perevalov V, Perrin A, Polovtseva ER, Richard C, Smith MAH, Starikova E, Sung K, Tashkun S, Tennyson J, Toon GC, Tyuterev VG, Wagner G. The *HITRAN* 2012 molecular spectroscopic database. J Quant Spectrosc Radiat Transf 2013;130:4–50. doi:10.1016/jqsrt.2013.07.002.
[86] Gordon IE, Rothman LS, Hill C, Kochanov RV, Tan Y, Bernath PF, Birk M, Boudon V, Campargue A, Chance KV, Drouin BJ, Flaud JM, Gamache RR, Hodges JT, Jacquemart D, Perevalov VI, Perrin A, Shine KP, Smith MAH, Tennyson J, Toon GC, Tran H, Tyuterev VG, Barbe A, Császár AG, Devi VM, Furtenbacher T, Harrison JJ, Hartmann JM, Jolly A, Johnson TJ, Karman T, Kleiner I, Kyuberis AA, Loos J, Lyulin OM, Massie ST, Mikhailenko SN, Moazzen-Ahmadi N, Müller HSP, Naumenko OV, Nikitin AV, Polyansky OL, Rey M, Rotger M, Sharpe SW, Sung K, Starikova E, Tashkun SA, Vander Auwera J, Wagner G, Wilzewski J, Wcisło P, Yu S, Zak EJ. The *HITRAN* 2016 molecular spectroscopic database. J Quant Spectrosc Radiat Transf 2017;203:3–69. doi:10.1016/j.jqsrt.2017.06.038.
[87] Rothman L, Gamache RR, Tipping RH, Rinsland CP, Smith MAH, Benner DC, Devi VM, Flaud JM, Camy-Peyret C, Perrin A, Goldman A, Massie ST, Brown LR, Toth RA. The HITRAN molecular database - editions of 1991 and 1992. J Quant Spectrosc Radiat Transf 1992;48:469–507. doi:10.1016/0022-4073(92)90115-K.
[88] Rothman LS, Barbe A, Benner DC, Brown LR, Camy-Peyret C, Carleer MR, Chance K, Clerbaux C, Dana V, Devi VM, Fayt A, Flaud JM, Gamache RR, Goldman A, Jacquemart D, Jucks KW, Lafferty WJ, Mandin JY, Massie ST, Nemtchinov V, Newnham DA, Perrin A, Rinsland CP, Schroeder J, Smith KM, Smith MAH, Tang K, Toth RA, Auwera JV, Varanasi P, Yoshino K. The HITRAN molecular spectroscopic database: edition of 2000 including updates through 2001. J Quant Spectrosc Radiat Transf 2003;82:5–44. doi:10.1016/S0022-4073(03)00146-8.
[89] Rothman LS, Jacquemart D, Barbe A, Benner DC, Birk M, Brown LR, Carleer MR, Chackerian C, Chance K, Coudert LH, Dana V, Devi VM, Flaud JM, Gamache RR, Goldman A, Hartmann JM, Jucks KW, Maki AG, Mandin JY, Massie ST, Orphal J, Perrin A, Rinsland CP, Smith MAH, Tennyson J, Tolchenov RN, Toth RA, Auwera JV, Varanasi P, Wagner G. The *HITRAN* 2004 molecular spectroscopic database. J Quant Spectrosc Radiat Transf 2005;96:139–204.
[90] Rothman LS, Gordon IE, Barbe A, Benner DC, Bernath PF, Birk M, Boudon V, Brown LR, Campargue A, Champion JP, Chance K, Coudert LH, Dana V, Devi VM, Fally S, Flaud JM, Gamache RR, Goldman A, Jacquemart D, Kleiner I, Lacome N, Lafferty WJ, Mandin JY, Massie ST, Mikhailenko SN, Miller CE, Moazzen-Ahmadi N, Naumenko OV, Nikitin AV, Orphal J, Perevalov VI, Perrin A, Predoi-Cross A, Rinsland CP, Rotger M, Simeckova M, Smith MAH, Sung K, Tashkun SA, Tennyson J, Toth RA, Vandaele AC, Auwera JV. The *HITRAN* 2008 molecular spectroscopic database. J Quant Spectrosc Radiat Transf 2009;110:533–72.
[91] Azzam AAA, Yurchenko SN, Tennyson J, Naumenko OV. Exomol line lists XVI: A hot line list for $H_2s$. Mon Not R Astron Soc 2016;460:4063–74. doi:10.1093/mnras/stw1133.
[92] Tennyson J, Yurchenko SN. Exomol: molecular line lists for exoplanet and other atmospheres. Mon Not R Astron Soc 2012;425:21–33. doi:10.1111/j.1365-2966.2012.21440.x.
[93] Tennyson J, Yurchenko SN, Al-Refaie AF, Barton EJ, Chubb KL, Coles PA, Diamantopoulou S, Gorman MN, Hill C, Lam AZ, Lodi L, McKemmish LK, Na Y, Owens A, Polyansky OL, Rivlin T, Sousa-Silva C, Underwood DS, Yachmenev A, Zak E. The exomol database: molecular line lists for exoplanet and other hot atmospheres. J Mol Spectrosc 2016;327:73–94. doi:10.1016/j.jms.2016.05.002.
[94] Barber RJ, Strange JK, Hill C, Polyansky OL, Mellau GC, Yurchenko SN, Tennyson J. Exomol line lists–III. An improved hot rotation-vibration line list for HCN and HNC. Mon Not R Astron Soc 2014;437:1828–35. doi:10.1093/mnras/stt2011.
[95] McKemmish LK, Chubb KL, Rivlin T, Baker JS, Gorman MN, Heward A, Dunn W, Tessenyi M. Bringing pupils into the ORBYTS of research. Astron Geophys 2017;58(5):5.11. doi:10.1093/astrogeo/atx169.
[96] Sousa-Silva C, McKemmish LK, Chubb KL, Baker J, Barton EJ, Gorman MN, Rivlin T, Tennyson J. Original research by young twinkle students (ORBYTS): when can students start performing original research? Phys Educ 2018;53:015020. doi:10.1088/1361-6552/aa8f2a.